


 Cite this: *RSC Adv.*, 2025, **15**, 16968

## CP/MAS NMR studies on binding environment of $\text{CH}_3\text{CN}$ in Cu(i) complexes with disilane-bridged bis(methylpyridine) ligands†

 Kei-ichi Sato,<sup>a</sup> Mineyuki Hattori  <sup>\*a</sup> and Yoshinori Yamanoi  <sup>\*b</sup>

CP/MAS NMR spectroscopies have developed as an important tool for studying the structure in the crystalline state. In this work, the structures of representative Cu(i) complexes **1–3** with disilane-bridged bis(methylpyridine) ligands in the crystalline state were investigated by CP/MAS NMR.  $^{13}\text{C}$  CP/MAS NMR confirmed the presence of  $\text{CH}_3\text{CN}$  in the crystals of **2** and **3**, but the environment around  $\text{CH}_3\text{CN}$  could not be determined. Natural abundance (ca. 0.36%)  $^{15}\text{N}$  CP/MAS NMR measurements could confirm the difference of  $\text{CH}_3\text{CN}$  environment between coordinating solvent in **2** and crystal solvent in **3**. The  $^{15}\text{N}$  CP/MAS of  $\text{CH}_3\text{CN}$  in **3** shows a singlet because it is not coordinated to Cu(i) and the crystal structure is stabilized by multiple intermolecular interactions. These data have provided valuable information on Cu(i) coordination environment, which was in good accordance with single-crystal X-ray analysis.

 Received 28th April 2025  
 Accepted 10th May 2025

 DOI: 10.1039/d5ra02962g  
[rsc.li/rsc-advances](http://rsc.li/rsc-advances)

## Introduction

Flexible molecular structures are known to induce crystalline polymorphism. The transition between the stable and metastable polymorphs triggered through external stimuli can induce alternation of photophysical properties.<sup>1,2</sup> Among them, investigations on the relationship between structure and properties of Cu(i) complexes are of significant interest.<sup>3–6</sup> Copper(i) complexes have been shown to be excellent candidates for solid-state emitters due to their high earth-abundance and low cost, coupled with their ability of bright luminescence at rt, resulting in complexes with interesting photophysical characteristics. These compounds have been found to exhibit a variety of structures from mononuclear to polynuclear copper complexes. Recently, we reported the synthesis and photophysical properties of Cu(i) complexes with disilane-bridged dipyridine ligands. Some compounds showed responsiveness under external stimuli in the crystalline state.<sup>7</sup>

Solid-state NMR is a non-destructive measurement method, and various information can be obtained by the measurement.<sup>8–12</sup> Especially, CP/MAS NMR spectroscopy can provide information about the structure and bonding of metal complexes in the crystalline state. Recently, the techniques have been developed to

improve resolution by rotating at high speeds.<sup>13</sup>  $^{13}\text{C}$  and  $^{15}\text{N}$  CP/MAS NMR, along with single-crystal X-ray structure analysis, are powerful techniques for structural analysis.<sup>14–17</sup>

The major difficulty in employing  $^{15}\text{N}$  NMR spectroscopy lies in its sensitivity, which is very low due to the low natural abundance (0.36%) of the  $^{15}\text{N}$  isotope. Although nitrogen-15 labelling compounds were used to employ  $^{15}\text{N}$  CP/MAS NMR,  $^{15}\text{N}$  NMR can be measured even for unlabelled  $^{15}\text{N}$  compounds by increasing accumulation numbers and using high-resolution NMR. Recently, we measured  $^{15}\text{N}$  CP/MAS NMR to track structural changes of organosilicon compounds upon mechanical stimulation.<sup>18</sup>

Cu complexes often decompose in solution, requiring solid-state NMR measurements. Previously, we reported the synthesis and optical properties of several Cu(i) complexes.<sup>19</sup> The  $^{13}\text{C}$  CP/MAS NMR of **2** and **3** showed the peaks of  $\text{CH}_3\text{CN}$  as similar chemical shift, and it was impossible to distinguish existence state between the crystal solvent and coordinated ligand.  $^{15}\text{N}$  CP/MAS NMR of transition metal complexes were measured to distinguish binding mode of  $\text{CH}_3\text{CN}$ . As Cu(i) complex, several  $^{15}\text{N}$  CP/MAS NMR of Cu(i) complexes were reported in natural abundance.<sup>20–23</sup> However little clear evidence has been given on the effect of metal binding to the  $^{15}\text{N}$  nuclear shielding constants.<sup>24–27</sup> In this paper, we used natural abundance  $^{15}\text{N}$  CP/MAS NMR to study binding mode of  $\text{CH}_3\text{CN}$  in Cu(i) complexes **1–3** (Fig. 1).

## Experimental section

### Materials

All chemicals and reagents were obtained from commercial sources and used without additional purification.

<sup>a</sup>National Institute of Advanced Industrial Science and Technology, AIST Central 5, 1-1 Higashi, Tsukuba, Ibaraki 305-8565, Japan. E-mail: [mineyuki.hattori@aist.go.jp](mailto:mineyuki.hattori@aist.go.jp)

<sup>b</sup>Department of Chemistry, School of Science, The University of Tokyo, 7-3-1 Hongo, Bunkyo-ku, Tokyo 113-0033, Japan. E-mail: [yamanoi@chem.s.u-tokyo.ac.jp](mailto:yamanoi@chem.s.u-tokyo.ac.jp)

† Electronic supplementary information (ESI) available: ORTEP drawings of **1–3** and crystal packing of **3**. CCDC 2339248, 2419410 and 2419411. For ESI and crystallographic data in CIF or other electronic format see DOI: <https://doi.org/10.1039/d5ra02962g>



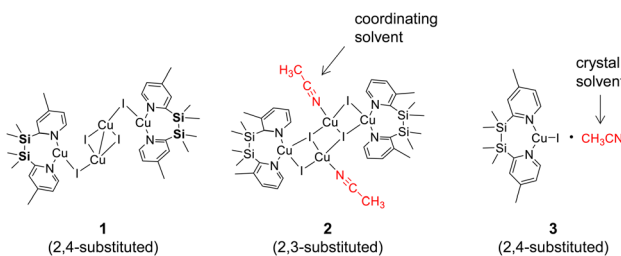


Fig. 1 Chemical structures of copper complexes **1–3** studied in this work.

1,1,2,2-Tetramethyl-1,2-bis(4-methylpyridin-2-yl)disilane and 1,1,2,2-tetramethyl-1,2-bis(3-methylpyridin-2-yl)disilane were prepared according to our previous report.<sup>7</sup>

### Synthesis of **1**

CuI (380 mg, 2.0 mmol) and 1,1,2,2-tetramethyl-1,2-bis(4-methylpyridin-2-yl)disilane (300 mg, 1.0 mmol) were dissolved in CH<sub>3</sub>CN (40 mL) at rt. The resulting yellow mixture was stirred at rt for 12 h. The solvent was evaporated under reduced pressure and the residue was washed with diethyl ether to give **1** as pale yellow crystalline solid. The solid was recrystallized from CH<sub>3</sub>CN to obtain analytically pure complex **1** as colorless cubes. Yield: 42% (290 mg). Elemental analysis. Calcd for C<sub>32</sub>H<sub>48</sub>N<sub>4</sub>Cu<sub>4</sub>I<sub>4</sub>Si<sub>4</sub>: C, 28.20; H, 3.55; N, 4.11. Found: C, 28.47; H, 3.53; N, 4.24.

### Synthesis of **2**

CuI (380 mg, 2.0 mmol) and 1,1,2,2-tetramethyl-1,2-bis(3-methylpyridin-2-yl)disilane (300 mg, 1.0 mmol) were dissolved in CH<sub>3</sub>CN (40 mL) at rt. The resulting yellow mixture was stirred at rt for 12 h. The solvent was evaporated under reduced pressure and the residue was washed with diethyl ether to give **2** as pale yellow crystalline solid. The solid was recrystallized from CH<sub>3</sub>CN to obtain analytically pure complex **2** as yellow cubes. Yield: 44% (305 mg). Elemental analysis. Calcd for C<sub>36</sub>H<sub>54</sub>N<sub>6</sub>Cu<sub>4</sub>I<sub>4</sub>Si<sub>4</sub>: C, 29.92; H, 3.77; N, 5.82. Found: C, 29.76; H, 3.70; N, 5.78.

### Synthesis of **3**

CuI (190 mg, 1.0 mmol) in CH<sub>3</sub>CN (15 mL) was added dropwise to a solution of 1,1,2,2-tetramethyl-1,2-bis(4-methylpyridin-2-yl)disilane (300 mg, 1.0 mmol) in CH<sub>3</sub>CN (5 mL) over 5 min at rt. After stirring at rt for 10 min, **3** was obtained as a yellow crystalline solid (314 mg, 60%). The solid was recrystallized from CH<sub>3</sub>CN to obtain analytically pure complex **3** as colorless cubes. The spectroscopic data were identical to our previous reported data.<sup>19</sup>

### Single-crystal X-ray structural analyses

All single-crystal X-ray diffraction measurements were conducted using a Rigaku Mercury CCD diffractometer with graphite-monochromated Mo K $\alpha$  radiation ( $\lambda = 0.71073 \text{ \AA}$ ) and a rotating-anode generator. Each crystal was mounted on a loop

using paraffin oil. Diffraction data were collected at around 100 K and processed using the Crystal Clear program. Structures were solved by direct methods using SIR-2011. Structural refinements were conducted by the full-matrix least-squares method using SHELXL-2013. All non-H atoms were refined anisotropically, and all H atoms were refined using the riding model. All calculations were performed using the Crystal Structure crystallographic software package. The crystallographic data were deposited in the Cambridge Crystallographic Data Centre.

### Crystallographic data for **1**

C<sub>32</sub>H<sub>48</sub>Cu<sub>4</sub>I<sub>4</sub>N<sub>4</sub>Si<sub>4</sub>, crystal dimensions: 0.15 mm × 0.15 mm × 0.05 mm.  $M = 1362.86$ , monoclinic,  $P12_1/n1$ ,  $a = 9.8145(5) \text{ \AA}$ ,  $b = 14.0010(8) \text{ \AA}$ ,  $c = 16.7363(10) \text{ \AA}$ ,  $\alpha = 90^\circ$ ,  $\beta = 98.366(2)^\circ$ ,  $\gamma = 90^\circ$ ,  $V = 2275.3(2) \text{ \AA}^3$ ,  $Z = 2$ ,  $T = 109 \text{ K}$ ,  $D_{\text{calc}} = 1.989 \text{ g cm}^{-3}$ ,  $F_{000} = 1304.0$ ,  $\lambda = 0.71073 \text{ \AA}$  (Mo K $\alpha$ ),  $\mu = 4.690 \text{ mm}^{-1}$ ,  $R_1 = 0.0177$  ( $I > 2\sigma(I)$ ),  $wR_2 = 0.0462$  (all data). GOF = 1.063. CCDC 2419410.

### Crystallographic data for **2**

C<sub>36</sub>H<sub>54</sub>Cu<sub>4</sub>I<sub>4</sub>N<sub>6</sub>Si<sub>4</sub>, crystal dimensions: 0.15 mm × 0.15 mm × 0.05 mm.  $M = 1444.97$ , triclinic,  $P\bar{1}$ ,  $a = 9.3981(5) \text{ \AA}$ ,  $b = 10.1021(6) \text{ \AA}$ ,  $c = 14.9219(8) \text{ \AA}$ ,  $\alpha = 81.667(2)^\circ$ ,  $\beta = 74.599(1)^\circ$ ,  $\gamma = 64.227(1)^\circ$ ,  $V = 1229.25(12) \text{ \AA}^3$ ,  $Z = 1$ ,  $T = 112 \text{ K}$ ,  $D_{\text{calc}} = 1.952 \text{ g cm}^{-3}$ ,  $F_{000} = 696.0$ ,  $\lambda = 0.71073 \text{ \AA}$  (Mo K $\alpha$ ),  $\mu = 4.348 \text{ mm}^{-1}$ ,  $R_1 = 0.0340$  ( $I > 2\sigma(I)$ ),  $wR_2 = 0.0706$  (all data). GOF = 1.036. CCDC 2419411.

### Crystallographic data for **3**

C<sub>18</sub>H<sub>27</sub>CuIN<sub>3</sub>Si<sub>2</sub>, crystal dimensions: 0.15 mm × 0.13 mm × 0.05 mm.  $M = 532.04$ , orthorhombic,  $Pca2_1$ ,  $a = 16.7137(6) \text{ \AA}$ ,  $b = 10.0411(3) \text{ \AA}$ ,  $c = 13.9102(5) \text{ \AA}$ ,  $\alpha = 90^\circ$ ,  $\beta = 90^\circ$ ,  $\gamma = 90^\circ$ ,  $V = 2334.46(14) \text{ \AA}^3$ ,  $Z = 4$ ,  $T = 100 \text{ K}$ ,  $D_{\text{calc}} = 1.514 \text{ g cm}^{-3}$ ,  $F_{000} = 1064.0$ ,  $\lambda = 0.71073 \text{ \AA}$  (Mo K $\alpha$ ),  $\mu = 2.367 \text{ mm}^{-1}$ ,  $R_1 = 0.0221$  ( $I > 2\sigma(I)$ ),  $wR_2 = 0.0431$  (all data). GOF = 1.033. CCDC 2339248.

### CP/MAS NMR spectroscopy

The sample was packed into a 4 mm zirconia rotor and measured with <sup>13</sup>C and <sup>15</sup>N cross-polarization/magic angle spinning (CP/MAS) NMR using a spectrometer (Bruker AVANCE III HD 600WB) at a Larmor frequency of 150.97 MHz (<sup>13</sup>C) and 60.86 MHz (<sup>15</sup>N). Bruker MAS probe head (MAS4DR) was used with a HR-MAS rotor with 4 mm diameter (HZ05538) and Teflon insert (50  $\mu\text{L}$ ), and sample spin rates were 10 kHz for <sup>13</sup>C and 8 kHz for <sup>15</sup>N, respectively. The chemical shifts refer to tetramethylsilane (<sup>13</sup>C) and nitromethane (<sup>15</sup>N) at 0.00 ppm. Glycine was used as a second reference material for <sup>13</sup>C NMR, and its carbonyl signal was set at 176.46 ppm. NH<sub>4</sub>Cl (10 atom% <sup>15</sup>N) was used as a second reference material for <sup>15</sup>N NMR, which was set at -341.15 ppm. The samples were measured at ambient probe temperature.

## Results and discussion

The <sup>13</sup>C CP/MAS NMR can be used to correlate solution NMR data and X-ray structure data.<sup>28</sup> <sup>13</sup>C CP/MAS NMR and X-ray



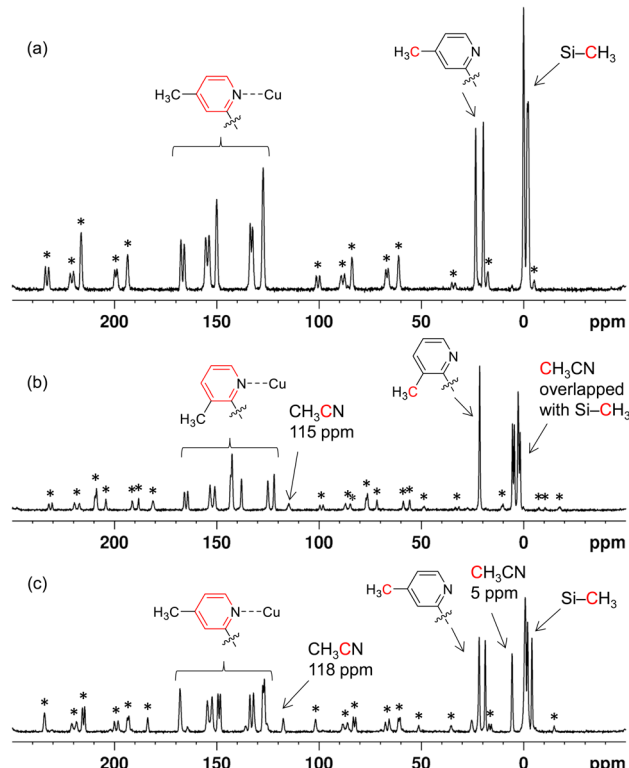


Fig. 2  $^{13}\text{C}$  CP/MAS NMR (151 MHz, 10 kHz MAS). (a) 1, (b) 2, and (c) 3. The parameters of CP/MAS are as follows: CP contact time: 2 ms, recycle delay: 8 s, and the number of scans: 2000. The signals with asterisks indicate spinning side band.

analysis are shown in Fig. 2 and S1,<sup>†</sup> respectively. Chemical shifts are sensitive to the surrounding environment, and hence obvious changes can be found in different structures. In the solid-state spectra of copper complex 1, we observed a number of peaks than the number of chemically distinct carbon atoms in the molecules (Fig. 2(a)). The doublet-like signals with the intensity ratio of *ca.* 1 : 1 observed in some peaks of  $^{13}\text{C}$  CP/MAS NMR spectra arise due to structurally nonequivalent carbon of the complex in the unit cell.

$^{13}\text{C}$  CP/MAS NMR reflects the unsymmetrized ligand molecule by crystallization and  $\text{CH}_3\text{CN}$  molecules.  $^{13}\text{C}$  CP/MAS of 2 shows signals of  $\text{CH}_3\text{CN}$  at 115 ppm ( $\text{CH}_3\text{CN}$ ) and around 5 ppm ( $\text{CH}_3\text{CN}$ , overlapped with  $\text{Si-CH}_3$ ) (Fig. 2(b)). The signal at 118 ppm and 5 ppm is attributed to the  $^{13}\text{C}$  peaks of  $\text{CH}_3\text{CN}$  in the crystal of 3 (Fig. 2(c)). However,  $^{13}\text{C}$  CP/MAS NMR did not show obvious information based on structural differences on  $\text{CH}_3\text{CN}$  between 2 and 3.

Nitrogen is a constituent of many ligands which are important in coordination chemistry. Natural abundance  $^{15}\text{N}$  CP/MAS NMR has been reported as a novel tool for investigating molecular information. Particularly, it is possible to consider the structure of metal complexes, and the  $^{15}\text{N}$  chemical shifts are sensitive to the coordinating or uncoordinating N atoms. Therefore, we measured  $^{15}\text{N}$  CP/MAS NMR of these copper complexes 1–3.

When the  $^{15}\text{N}$  NMR of copper complex 1 without  $\text{CH}_3\text{CN}$  was measured in the crystalline state, multiple peaks were observed

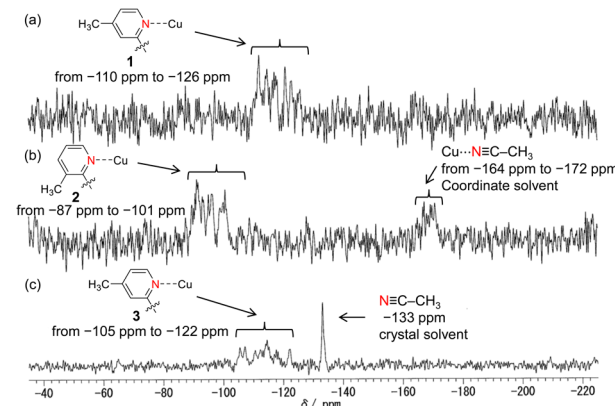


Fig. 3 Natural abundance  $^{15}\text{N}$  CP/MAS NMR (61 MHz, 8 kHz MAS). (a) 1, (b) 2, and (c) 3. The parameters of CP/MAS are as follows: CP contact time: 5 ms, recycle delay: 10 s, and the number of scans: (a) 8000, (b) 12 000, and (c) 12 000.

at from  $-110$  ppm to  $-126$  ppm, which were assigned as  $^{15}\text{N}$  of pyridine moiety (Fig. 3(a)). The  $^{15}\text{N}$  chemical shift was consistent with the results in analogous systems in solution.<sup>29–33</sup>  $^{15}\text{N}$  resonance of the free pyridine-based ligand showed at around  $-70$  ppm while the coordination of the pyridine to Cu(i) in solution showed the resonance at around  $-100$  ppm in the  $^{15}\text{N}$  NMR.<sup>34</sup> The complicated peaks in the solid state are due to not only the unsymmetrization observed in  $^{13}\text{C}$  spectra but also coupling between  $^{15}\text{N}$  and  $^{63}\text{Cu}/^{65}\text{Cu}$  nuclei. In a similar system,  $^{31}\text{P}$  CP/MAS NMR of Cu(i) complexes having phosphine ligands show complicated peaks due to coupling between the  $^{31}\text{P}$  and  $^{63}\text{Cu}/^{65}\text{Cu}$ .<sup>35,36</sup>

Complexes 2 and 3 contain one  $\text{CH}_3\text{CN}$ , which exist in different states in the crystal.  $^{15}\text{N}$  NMR chemical shifts are sensitive to the environment of N moiety. Therefore, detectability of  $\text{CH}_3\text{CN}$  in crystals is discussed by CP/MAS  $^{15}\text{N}$  NMR for identifying specific chemical functional groups.

$^{15}\text{N}$  CP/MAS NMR of 2 was shown in Fig. 3(b). The multiple peaks from  $-87$  ppm to  $-101$  ppm were  $^{15}\text{N}$  chemical shifts of pyridine ligands in 2. The chemical shift moved to the down-field side in comparison with 1 are due to the difference in the substitution position of the methyl group on pyridine ring. The  $^{15}\text{N}$  resonance of  $\text{CH}_3\text{CN}$  in 2 was also observed as multiple peaks from  $-164$  ppm to  $-172$  ppm. The chemical shift in the characteristic  $^{15}\text{N}$  resonance was observed upon  $N$ -cyano coordination to Cu(i) *via*  $\text{Cu}\cdots\text{N}\equiv\text{C-CH}_3$  interactions.

CP/MAS  $^{15}\text{N}$  NMR of 3 was measured (Fig. 3(c)). The multiple peaks from  $-105$  ppm to  $-122$  ppm were assigned to  $^{15}\text{N}$  of pyridine ring coordinated to Cu(i).  $^{15}\text{N}$  peak of  $\text{CH}_3\text{CN}$  molecules as the crystal solvent was observed at  $-133$  ppm as a sharp peak, which was lower field relative to 2. The  $\text{CH}_3\text{CN}$  peak of 3 is sharp because  $\text{CH}_3\text{CN}$  molecules have no  $\text{Cu}\cdots\text{N}$  interaction in the crystalline state. Although these results on  $\text{CH}_3\text{CN}$  binding mode agree with X-ray structures of 2 and 3, single crystal X-ray determinations are not always available for analysing the structure. The structures can often not be determined by Rietveld analysis of microcrystals. There is a need for alternative



spectroscopic methods to determine the ligand coordination mode.  $^{15}\text{N}$  CP/MAS NMR is a valuable tool for distinguishing the binding environments in the crystals. This study provides spectroscopic support for insight into the coordination mode of solvent in metal complexes.

$\text{CH}_3\text{CN}$  molecules in **2** exist in the crystal through a coordination bond with  $\text{Cu}(\text{i})$  ( $\text{CH}_3\text{C}\equiv\text{N}\cdots\text{Cu}$ ), and  $\text{CH}_3\text{CN}$  molecules in **3** exist through hydrogen bonds between N lone pair of  $\text{CH}_3\text{CN}$  and aromatic proton ( $\text{CH}_3\text{C}\equiv\text{N}\cdots\text{H-Ar}$ ) (Fig. S2†). The  $^{15}\text{N}$  NMR peak shapes of  $\text{CH}_3\text{CN}$  change depending on the coordination or uncoordination with  $\text{Cu}(\text{i})$ .  $^{15}\text{N}$  NMR peaks of  $\text{CH}_3\text{CN}$  in **2** are complicated by the coupling between  $^{15}\text{N}$  and  $^{63}\text{Cu}$  nuclei due to the coordination of  $\text{CH}_3\text{CN}$  to  $\text{Cu}(\text{i})$ . On the other hand, there is no interaction between  $\text{CH}_3\text{CN}$  and  $\text{Cu}(\text{i})$  in the crystal of **3**, and  $^{15}\text{N}$  NMR peak of  $\text{CH}_3\text{CN}$  is observed as a sharp singlet.

## Conclusion

This work describes detailed structural information on  $\text{Cu}(\text{i})$  complexes in the crystalline state using natural abundance  $^{15}\text{N}$  CP/MAS NMR.  $^{13}\text{C}$  and  $^{15}\text{N}$  CP/MAS NMR spectra of **1–3** were in accord with the direct structural data on the complexes.  $\text{CH}_3\text{CN}$  in these complexes has restricted molecular motion in single crystals and could be observed by CP/MAS NMR.<sup>37</sup> Natural abundance  $^{15}\text{N}$  CP/MAS NMR spectra provided considerable information on the crystalline state, because the state of the solvents contained can be deduced from NMR spectroscopy in addition to single crystal X-ray structure analysis.  $^{15}\text{N}$  NMR peak shapes of these  $\text{Cu}(\text{i})$  complexes are related to the environment of the nitrogen atoms in the crystal. The differences between coordinated and uncoordinated  $\text{CH}_3\text{CN}$  were able to be distinguished by  $^{15}\text{N}$  CP/MAS NMR. Molecular packing had an impact on the splitting patterns and peak shapes of the  $^{15}\text{N}$  peak of  $\text{CH}_3\text{CN}$ .

The  $^{15}\text{N}$  chemical shift and peak shape were sensitive to cyanide interactions observed in  $\text{Cu}(\text{i})$  complexes. Sharp  $^{15}\text{N}$  signal was observed corresponding to  $\text{CH}_3\text{CN}$  of crystal solvent with the stabilization of multiple intermolecular interactions. On the contrary, multiple  $^{15}\text{N}$  signals of  $\text{CH}_3\text{CN}$  was observed corresponding to  $\text{Cu}\cdots\text{N}\equiv\text{C-CH}_3$  interactions. These observations suggest a detailed study of solvent environments in the crystal.

## Data availability

The data supporting this article have been included as part of the ESI.†

## Conflicts of interest

There are no conflicts to declare.

## Acknowledgements

This work was financially supported by Grant-in-Aids for Scientific Research (C) (no. JP22K05250 and JP25K08585) from

the Ministry of Education, Culture, Sports, Science, and Technology, Japan. Solid state NMR measurements were supported by AIST Nanocharacterization Facility (ANCF) in the Nanotechnology Platform Project (no. JPMXP1224AT5010) sponsored by the Ministry of Education, Culture, Sports, Science and Technology (MEXT), Japan.

## Notes and references

- M. Kato, H. Ito, M. Hasegawa and K. Ishii, Soft Crystals: Flexible Response Systems with High Structural Order, *Chem.-Eur. J.*, 2019, **25**, 5105–5112.
- Soft Crystals: Flexible Response Systems with High Structural Order*, ed. M. Kato and K. Ishii, Springer, Singapore, 2023.
- A. Kobayashi and M. Kato, Stimuli-responsive luminescent copper(I) complexes for intelligent emissive devices, *Chem. Lett.*, 2017, **46**, 154–162.
- P. Naumov, S. Chizhik, M. K. Panda, N. K. Nath and E. Boldyreva, Mechanically responsive molecular crystals, *Chem. Rev.*, 2015, **115**, 12440–12490.
- M. Kato, Luminescent copper(I) complexes exhibiting chromic phenomena, *J. Crystallogr. Soc. Jpn.*, 2015, **57**, 110–115.
- P. C. Ford, E. Cariati and J. Bourassa, Photoluminescence properties of Multinuclear copper(I) compounds, *Chem. Rev.*, 1999, **99**, 3625–3648.
- Y. Zhao, T. Nakae, M. Hattori, M. Yoshida, M. Kato, K. Omoto, S. Ito and Y. Yamanoi, Structural and photophysical studies of copper iodide clusters coordinated with disilane-bridged bis(methylpyridine) ligands, *Chem.-Eur. J.*, 2023, **29**, e202204002.
- T. Molugu, S. Lee and M. Brown, Concepts and methods of solid-state NMR spectroscopy applied to biomembranes, *Chem. Rev.*, 2017, **117**, 12087–12132.
- C. S. Yannoni, High-Resolution NMR in Solids: The CPMAS Experiment, *Acc. Chem. Res.*, 1982, **15**, 201–208.
- M. Mehring, *Principals of High Resolution NMR in Solids*, Springer-Verlag, Berlin, 2nd edn, 1983.
- Solid-state NMR: Principles and Applications*, ed. M. J. Duer, Blackwell Science, Oxford, 2002.
- H. Saitô, I. Ando and A. Ramamoorthy, Chemical shift tensor – The heart of NMR: insights into biological aspects of proteins, *Prog. Nucl. Mag. Res. Spectrosc.*, 2010, **57**, 181–228.
- Y. Nishiyama, G. Hou, V. Agarwal, Y. Su and A. Ramamoorthy, Ultrafast Magic Angle Spinning Solid-State NMR Spectroscopy: Advances in Methodology and Applications, *Chem. Rev.*, 2023, **123**, 918–988.
- S. H. K. Hayamizu, Chemical Shift Standards in High-Resolution Solid-State NMR (2)  $^{15}\text{N}$  Nuclei, *Bull. Chem. Soc. Jpn.*, 1991, **64**, 688–690.
- M. Munowitz, W. W. Bachovchin, J. Herzfeld, C. M. Dobson and R. G. Griffin, Acid-Base and Tautomeric Equilibria in the Solid State:  $^{15}\text{N}$  NMR Spectroscopy of Histidine and Imidazole, *J. Am. Chem. Soc.*, 1982, **104**, 1192–1196.
- J. Mason, Nitrogen Nuclear Magnetic Resonance Spectroscopy in Inorganic, Organometallic, and Bioinorganic Chemistry, *Chem. Rev.*, 1981, **81**, 205–227.



17 Y. Yamanoi and M. Hattori, Recent progress on solid-state CP/MAS NMR measurements: A tool for investigating structural changes in stimuli-responsive organic compounds, *Bull. Chem. Soc. Jpn.*, 2024, **97**, uoad019.

18 T. Nakae, M. Hattori and Y. Yamanoi,  $^{15}\text{N}$  CP/MAS NMR as a Tool for the Mechanistic Study of Mechanical Stimuli-Responsive Materials: Evidence for the Conformational Change of an Emissive Dimethylacridane Derivative, *ACS Omega*, 2023, **8**, 12922–12927.

19 Y. Zhao, T. Nakae, K. Segawa, M. Yoshida, M. Kato, K. Omoto, S. Ito, T. Yamada and Y. Yamanoi, Structural and photophysical differences in crystalline trigonal planar copper iodide complexes with 1,2-bis(methylpyridine-2-yl) disilane ligands, *Inorg. Chem.*, 2024, **63**, 22361–22371.

20  $[\text{Cu}(\text{phen})_2]\text{PF}_6$ : S. Kitagawa, M. Munakata, K. Deguchi and T. Fujito, Natural Abundance Nitrogen-15 CP-MAS NMR Studies of Copper(I) Complexes, *Magn. Reson. Chem.*, 1991, **29**, 566–568.

21  $[\text{Cu}(\text{CN})_4]^{3-}$ : E. M. Poll, J. -U. Schütze, R. D. Fischer, N. A. Davies, D. C. Apperley and R. K. Harris, Self-assembly of  $[\text{Cu}(\text{CN})_4]^{3-}$  ions with cationic  $\{\text{Me}_3\text{Sn}\}^+$  or  $\{\text{Me}_2\text{Sn}(\text{CH}_2)_3\text{SnMe}_2\}^{2+}$  fragments in the presence of a  $^n\text{Bu}_4\text{N}^+$  template, *J. Organomet. Chem.*, 2001, **621**, 254–260.

22  $(\text{bpy})\text{Cu}\{\text{N}(\text{CF}_3)_2\}$ : L. N. Schneider, E. -M. T. Krauel, C. Deutsch, K. Urbahns, T. Bischof, K. A. M. Maibom, J. Landmann, F. Keppner, C. Kerpen, M. Hailmann, L. Zapf, T. Knuplez, R. Bertermann, N. V. Ignatev and M. Finze, Stable and Storable  $\text{N}(\text{CF}_3)_2$  Transfer Reagents, *Chem.-Eur. J.*, 2021, **27**, 10973–10978.

23 Cu-cryptand complex: M. G. B. Drew, D. Farrell, G. G. Morgan, V. McKee and J. Nelson,  $d^{10}$  Cations within triple-helical cryptand hosts; a structural and modelling study, *J. Chem. Soc., Dalton Trans.*, 2000, 1513–1519.

24 L. Pazderski,  $^{15}\text{N}$  and  $^{31}\text{P}$  NMR Coordination Shifts in Transition Metal Complexes with Nitrogen- and Phosphorus-Containing Heterocycles, *Annu. Rep. NMR Spectrosc.*, 2013, **80**, 33–179.

25 L. Pazderski,  $^{15}\text{N}$  NMR coordination shifts in transition metal complexes and organometallics with heterocycles containing nitrogen—update for 2012–20, *Annu. Rep. NMR Spectrosc.*, 2020, **101**, 151–284.

26 L. Pazderski, E. Szlyk, J. Sitkowski, B. Kamienski, L. Kozerski, J. Tousek and R. Marek, Experimental and quantum-chemical studies of  $^{15}\text{N}$  NMR coordination shifts in palladium and platinum chloride complexes with pyridine, 2,2'-bipyridine and 1,10-phenanthroline, *Magn. Reson. Chem.*, 2006, **44**, 163–170.

27 L. Pazderski,  $^{15}\text{N}$  NMR coordination shifts in Pd(II), Pt(II), Au(III), Co(III), Rh(III), Ir(III), Pd(IV), and Pt(IV) complexes with pyridine, 2,2'-bipyridine, 1,10-phenanthroline, quinoline, isoquinoline, 2,2'-biquinoline, 2,2':6',2'-terpyridine and their alkyl or aryl derivatives, *Magn. Reson. Chem.*, 2008, **46**, S3–S15.

28 *Encyclopedia of Nuclear Magnetic Resonance*, ed. D. M. Grant and R. K. Harris, Wiley, Baffins Lane, Chichester, 1995.

29 T. Ueda, S. Nagatomo, H. Masui, N. Nakamura and S. Hayashi, Hydrogen Bonds in Crystalline Imidazoles Studied by  $^{15}\text{N}$  NMR and ab initio MO Calculations, *Z. Naturforsch.*, 1999, **54**, 437–442.

30 P. Bertani, J. Raya and B. Bechinger,  $^{15}\text{N}$  chemical shift referencing in solid state NMR, *Solid State Nucl. Magn. Reason.*, 2014, **61–62**, 15–18.

31 J. C. Facelli and G. A. Webb, *Modern Magnetic Resonance*, ed. G. A. Webb, Springer, Dordrecht, The Netherlands, 2006, pp. 49–58.

32 R. Parr and W. Yang, *Density-functional Theory of Atoms and Molecules*, New York, 1989.

33 P. Wilson, Density Functional Theory and its Application to Nuclear Magnetic Resonance Shielding Constants, *Annu. Rep. NMR Spectrosc.*, 2003, **49**, 117.

34 R. Molteni, K. Edkins, M. Haehnel and A. Steffen, C–H Activation of Fluoroarenes: Synthesis, Structure, and Luminescence Properties of Copper(I) and Gold(I) Complexes Bearing 2-Phenylpyridine Ligands, *Organometallics*, 2016, **35**, 629–640.

35 A. Olivieri, Study of Quadrupole-Perturbed Quartets in the Solid-State Magic-Angle Spinning  $^{31}\text{P}$  NMR Spectra of Phosphine-Cu(I) Complexes.  $^{63}\text{Cu}$  Electric Field Gradients and Anisotropy in the  $^{31}\text{P}$ ,  $^{63}\text{Cu}$  Scalar Coupling, *J. Am. Chem. Soc.*, 1992, **114**, 5758–5763.

36 G. A. Bowmaker, S. E. Boyd, J. V. Hanna, R. D. Hart, P. C. Healy, B. W. Skelton and A. H. White, Structural and spectroscopic studies on three-coordinate complexes of copper(I) halides with tricyclohexylphosphine, *J. Chem. Soc., Dalton Trans.*, 2002, 2722–2730.

37 J. Schaefer, E. O. Stejskal and R. Buchdahl, Magic-Angle  $^{13}\text{C}$  NMR Analysis of Motion in Solid Glassy Polymers, *Macromolecules*, 1977, **10**, 384–405.

